



## Correlation between process and silica dispersion/distribution into composite: Impact on mechanical properties and Weibull statistical analysis

Alexandra Siot, Claire Longuet, Romain Léger, Belkacem Otazaghine, Patrick Ienny, Anne-Sophie Caro-Bretelle, Nathalie Azéma

### ► To cite this version:

Alexandra Siot, Claire Longuet, Romain Léger, Belkacem Otazaghine, Patrick Ienny, et al.. Correlation between process and silica dispersion/distribution into composite: Impact on mechanical properties and Weibull statistical analysis. *Polymer Testing*, 2018, 70, pp.92 - 101. 10.1016/j.polymertesting.2018.06.007 . hal-01908907

**HAL Id: hal-01908907**

**<https://hal.science/hal-01908907>**

Submitted on 30 Oct 2018

**HAL** is a multi-disciplinary open access archive for the deposit and dissemination of scientific research documents, whether they are published or not. The documents may come from teaching and research institutions in France or abroad, or from public or private research centers.

L'archive ouverte pluridisciplinaire **HAL**, est destinée au dépôt et à la diffusion de documents scientifiques de niveau recherche, publiés ou non, émanant des établissements d'enseignement et de recherche français ou étrangers, des laboratoires publics ou privés.

**Correlation between process and silica dispersion/distribution into composite:  
impact on mechanical properties and Weibull statistical analysis.**

Alexandra Siot, Claire Longuet\*, Romain Léger, Belkacem Otazaghine, Patrick Ienny,  
Anne-Sophie Caro-Bretelle and Nathalie Azéma

<sup>+</sup>*Centre des Matériaux des Mines d'Alès (C2MA), IMT Mines Alès, 6 Avenue de  
Clavières, 30319 Alès Cedex, France.*

\*[claire.longuet@mines-ales.fr](mailto:claire.longuet@mines-ales.fr), +33(0)466785345

*This article has been first published online in Polymer Testing, in June 15<sup>th</sup>, 2018.*

**Highlights:**

- Control and characterization of particles dispersion all along the elaboration process
- Highlighting the contribution of a good vs. poor particles dispersion on mechanical properties
- Weibull Theory : failure probability of composite as a function of inclusions dispersion and particle size

**Keywords:** Process dispersion, mechanical properties, Weibull theory, composite

**Abstract**

The aim of this study is to propose a methodology for controlling and monitoring particle dispersion at each step of composite manufacturing. Composites with well and poor particle dispersion were manufactured and characterized by numerous methods to estimate the impact of different dispersion state on mechanical properties. An original Weibull statistical analysis is suggested and shows the impact of this dispersion state on ultimate stress. For this purpose, a "model" matrix of PMMA was chosen. Well-dispersed silica enhanced Young's modulus by ~9% and ultimate stress by ~6%, while poorly-dispersed silica does not affect Young's modulus and ultimate stress. Moreover, a size effect is observed for well-dispersed composites; and not with poor particles dispersion.

## Introduction

Polymer composites are widely used in applications such as transportation, high technology, and electronics products thanks to very promising mechanical, thermal, and electrical properties [1–4]. Reinforcements used for composites can take many forms (particles, platelets, nanotubes...). Silica is one of the most representative particulate reinforcements, and is used to reinforce mechanical properties [5] or to improve flame retardancy of polymers [6,7]. One of the obstacles for the use of particles in polymer matrix is the poor control of its dispersion [8]. Even if for electrical properties, percolation is wanted [9], for mechanical properties, a good dispersion of particles is highly recommended. It is necessary to distinguish distribution and dispersion, in studies concerning particles repartition into a composite. The first one is limited to a homogeneous repartition of particles in a defined space. While, dispersion, try to access to single particles: isolated particles of each other's without the necessity of a homogeneous spatial repartition [10]. It is necessary to control the dispersion at each step of the process to ensure a good dispersion in the final composite, whether working in the molten or the solvent phase. The impact of the particles dispersion is highly studied in the literature for metallic and ceramic composites [11–13]. While, for organic composites, only few characterizations of the dispersion were found in the literature [14–17]. In these works, no comparison of same formulation with distinct dispersion state (well and poorly dispersed materials) were performed. To insure a well-dispersed composite, it is necessary to verify after every stage of the process that particles are not re-agglomerated. This is not always performed in the literature and constitutes, according to the authors, a lack. Nowadays, to our knowledge, there is no direct link between various dispersion states and final mechanical properties of composites while the interest of this dispersion was highlighted in various studies. Indeed, it is proven that the fillers agglomeration in the matrix causes premature failure of the composite [18–20] and lead, in some cases to decrease the composites Young's modulus [21]. Usually, most of the composites are a mix of isolated and agglomerated particles. To optimize the microstructure, it is necessary to characterize and control particles dispersion throughout the process of composite elaboration. One of the proposed methods to overcome the problem of dispersion in a given medium is to make them compatible. In this context, a lot of studies deal with the functionalization (e.g. silica in polymethylmethacrylate (PMMA) [22,23]; rubbers [24–26] ; Polyamide-imides (PAI)

[27]; Poly L lactic acid (PLLA) [28]), and in addition, to improve mechanical properties of composites. One of the drawbacks of this method is that it is not universal and has to be designed as a function of one particle for one medium.

Therefore, it is necessary to develop a dispersion method able to adapt to any medium and/or with any particles. In the literature, methods such as hot melt extrusion [29] (with optimized screw profile, melting time or screw speed), ultrasound (US) process [30–32] (generally in solution) are reported as promising solutions. According to these results this study has been focused on the using of US process.

To simplify the mechanical study it is important to choose a matrix without any nucleation or crystallization effects as described by Manias and al. [33]. An amorphous matrix is the best solution to avoid these structural modification problems. One of the most current polymers in the literature and thus used in this study, is the PMMA. This polymer is widely used as a substitute for inorganic glass thanks to its lightweight, transparency and ease of processing. The disadvantage of this material is its poor mechanical properties and many research groups have worked on the incorporation of inorganic fillers to this matrix in order to improve its physical properties [34–36]. In this study, in order to keep the PMMA transparency, filler content was fixed to 1wt%. This load percent is currently used to reach good mechanical properties [37–40]. In addition of load percent, a lot of studies deal with the effect of particles size. It is well known that the particle size influences the mechanical properties [41–43] especially the smallest ones with regards to Young's modulus [44]. Two submicronic particles sizes were thus synthesized in this work, in order to study a composite between a micro and a nanocomposite.

The aim of this paper was to study the impact of the process on the fillers dispersion and how this dispersion impacts the mechanical properties of PMMA-SiO<sub>2</sub> composites. Several models were elaborated, each of them showing a good (uniform particle) or a poor (high agglomeration) SiO<sub>2</sub> dispersion. This study wants to show by experiments and statistical study, that the particle dispersion quality has much more influence than the particle size on mechanical properties.

## **Experimental details**

### **1. Reagents**

PMMA was supplied by Arkema (Altuglass V825T) and used as received. Deionized water was used throughout this work. Acetone, tetraethoxysilane (TEOS, 98%) and ammonia (35%) were purchased from Merck Schuchardt OHG.

Ethanol was purchased from Sigma–Aldrich. All reagents were used as received without any further purification.

### **2. Particles synthesis**

Two silica particles powder were synthesized by a modified Stöber method already used in previous works [45,46].

Both synthesis reactions were performed in a 100 mL glass reactor. First synthesis used 26 g  $\text{NH}_3$  (25%) and 36 g pure water, injected into 212 g of pure ethanol (EtOH). Then, 20 g TEOS (silica precursor) was quickly added to the vial, while stirring at 50 °C for 10 h in view of the growth of silica.

For the second method, 24 g  $\text{NH}_3$  (25%); 18 g  $\text{H}_2\text{O}$  and 515 g EtOH are injected into the 100 mL glass reactor. Then, 20 g TEOS is added, while stirring at regulated room temperature (25 °C) for 2 days. Numerous studies have shown that all the process conditions, like the temperature, TEOS ratio or process time for example, have an important impact on the particles size [47–49]. Also, higher concentration of water resulted in larger size of the particle.

At the end of these two syntheses, ethanol was removed before use and replaced by water using evaporation under vacuum. Then, the dried silica was purified, in order to remove remaining reactants, by washing and centrifugation methods. First protocol has allowed to obtain 5.33 g (yield~92%) of silica with a size of 470nm (silica L), and second protocol 4.11 g (yield~71%) of silica with a size of 140nm (silica M).

### **3. Instrumentation and methods**

#### *Laser diffraction particle size analyzer*

The instrument used is a laser granulometer LS 13 320 from Beckman-Coulter Company. A scattering of monochromatic light ( $\lambda=780\text{nm}$ ) diffracted and transmitted through the suspension permits to obtain particle size distribution performed in acetone containing a few milligrams of silica powder. The optical model used for silica has been computed for a refractive index with a real part of 1.33 and an imaginary part of 1.5.

### *Zeta potential measurements*

Zeta Potentials ( $\zeta$ ) of particles were all measured at 25 °C using a Zetasizer Nano ZS (Malvern instruments Ltd., England) with a red laser (633 nm). DTS1060-folded capillary cell was used as the sample container. Three repeats for each sample were conducted to estimate the error in measurements. A titration machine (MPT-2 Malvern instruments Ltd.; England) was used in order to determinate the zeta potential function of pH. The titration procedure was carried out by increasing (from the solution pH to 13) with a 1M NaOH solution and decreasing (from the solution pH to 1) with a 1M HCl solution.

### *Scanning Electron Microscopy (SEM)*

SEM measurements were performed with an Environmental Scanning Electron Microscope with Energy Dispersive X-ray spectroscopy (ESEM–EDX) (Quanta 200 FEG) from the FEI Company.

Dispersion quality was investigated with this machine for the master-batch and the strand. To this end, the composites have been cut under nitrogen (freeze-fracture). Then, they were deposited on a sample holder with a carbon scotch and were metallized in high vacuum sputtering metallizer Bal-Tec CED 030 Balzers in order to ensure their stability during the analysis.

### *Mechanical properties*

Uniaxial tensile tests of composites PMMA/silica were performed on a tensile machine (Zwick/Roell) equipped with a 2.5kN load cell and a clip-on extensometer with a reference length of 30 mm at room temperature (25°C). A crosshead speed of 1 mm/min was applied. The Young's modulus was determined by tangent method between 0.05 and 0.25% of elongation. Each test was carried out at least 4 times.

## **4. Processes**

The composites were elaborated in three steps: the first one is the production of a PMMA/Silica master-batch, the second one is the dilution of this master-batch and the last one is the injection of the blend to obtain mechanical test specimens.

## 4.1 Master-batch formulations

Firstly, the synthesized silica particles were ultra-sonicated into suspension to reach several levels of dispersions. The most commonly used in the laboratories and investigated in this study are: a bath and a probe sonicator.

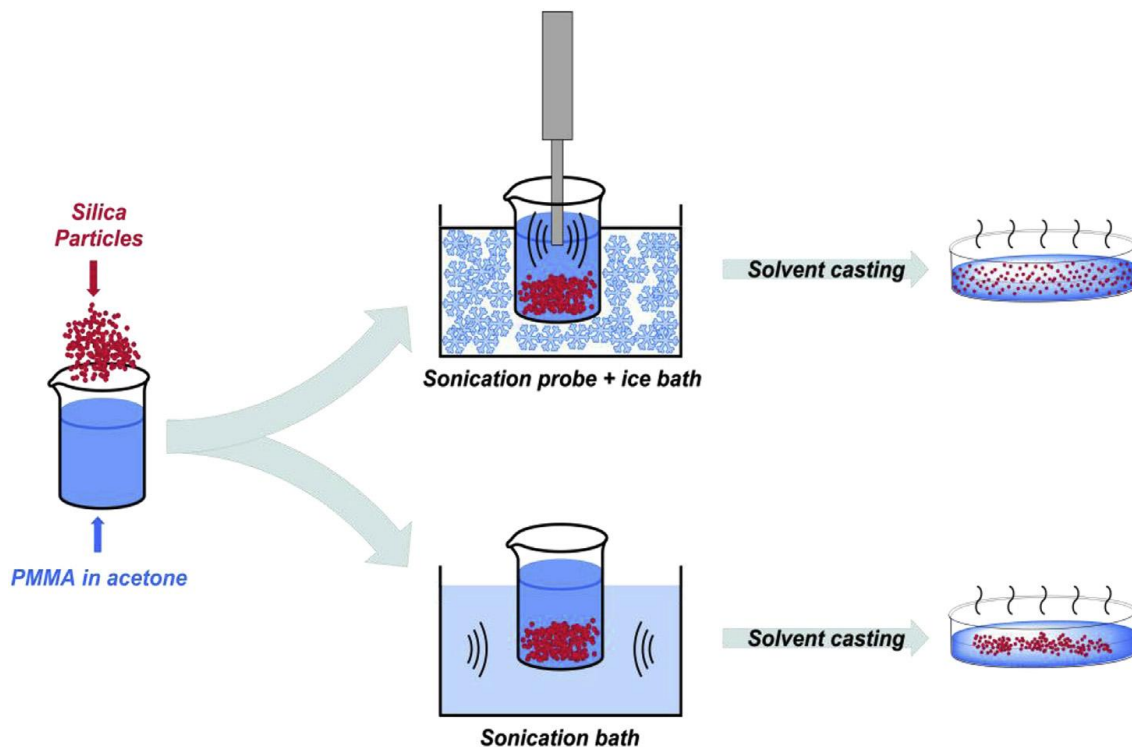


*Fig1. Two different approaches of the particles dispersion*

For the first procedure PMMA/silica/acetone suspension was introduced in a beaker (20mL) and sonicated using an ultrasonic bath.

For the second procedure silica/acetone suspension was introduced in a beaker (20mL) and sonicated using a probe. After dissolution of PMMA in acetone, the polymer was added to the dispersion and the solution was also sonicated.

Sonication times for both processes were chosen arbitrarily; 10 minutes for the first silica size and 65 minutes for the second one in order to reach an optimized dispersion.

The estimated power of bath and probe was respectively 240W and 59W.

After those dispersion processes, a film was obtained by a solvent casting procedure and dried at room temperature under a fume hood for 2 days.

## 4.2 Dilution method

The films obtained previously which exhibit several levels of silica dispersion (thanks to the processes described in the previous sections) were blended at molten state. 6.6g of PMMA was added with a twin screw compounder DSM<sup>®</sup>. To obtain a homogeneous

strand charged 1wt % silica, composites were blended at 250 °C for 4 minutes with a screw speed of 80 rpm.

### 4.3 Injection

The obtained strand was injected at 250 °C with an injection molding machine, Zamak Mercator with a molding pressure of 5 bar maintained for 10 seconds. We obtained ISO 527-2 type-1BA specimens for mechanical tests.

## 5. Statistical analysis: Weibull approach

The failure strength of several samples can be significantly different due to their microstructural heterogeneity. To analyze the statistical variation of the failure strength in such materials, Waloddi Weibull adopted in 1951 the statistics of extreme [50]. This approach uses a probability distribution function that characterizes the local failure strength. This law (equation 1) depends on the experimental ultimate stress  $\sigma_r$ , the shape parameter  $m$  (Weibull modulus) and the scale parameter or characteristic strength  $\sigma_0$ .

$$P_r = 1 - \exp \left\{ - \left( \frac{\sigma_r}{\sigma_0} \right)^m \right\} \quad (1)$$

The experimental fracture probability is defined by the relation:

$$P_r = \frac{k}{n+1} \quad (2)$$

where  $k$  is the rank in strength from least to greatest,  $n$  denotes the total number of samples.

Equation (1) can be rewritten as:

$$\ln[-\ln(1 - P_r)] = m \ln(\sigma_r) - m \ln(\sigma_0) \quad (3)$$

The Weibull modulus,  $m$ , characterizes the degree of homogeneity in the structure and so the degree of scattering of failure strength. A high  $m$  value corresponds to a homogeneous structure with a uniform strength, whereas a low value of the Weibull modulus indicates a high scattering of the measured parameters. Besides, the characteristic strength  $\sigma_0$  is a location parameter. Hence a straight line is expected between  $\ln(-\ln(1 - P_r))$  and  $\ln \sigma_r$  with slope  $m$ . From the value of  $m$  and intercept  $-m \ln \sigma_0$ , the value of  $\sigma_0$  can be determined.

Around 20 specimens were tested to obtain good estimates of the Weibull parameters. The samples that were not broken in the zone of interest were set aside.



## Results and discussions

### 1. Particles analysis and dispersion study

The obtained silica particles were observed by SEM (Fig2). Micrographs show monodisperse spherical particles with two different sizes: (a) 470 nm (silica L) and (b) 140 nm (silica M). For the silica L particles the TEOS/water ratio was approximately 1/2, for the silica M particles the ratio was 1/1. This result confirms the impact of water concentration. A TEOS/water ratio which is multiplied by two implies a three-fold increase of the final size of silica particles.

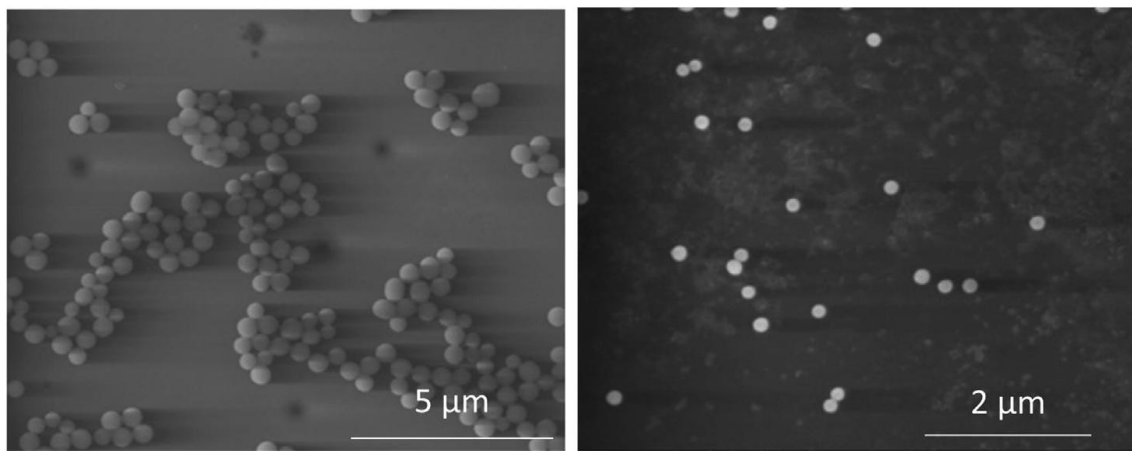


*Fig2. SEM micrographs of the synthesized (a) silica L and (b) silica M*

When NPs are in suspension they generally tend to agglomerate due to their high free surface energy [51,52]. Zeta-potential study was conducted to evaluate the particle dispersion. In order to optimize the silica dispersion, this study allowed the estimation of the suitable solution pH value knowing that a high zeta-potential predicts a good dispersion stability of particles [51,53]. Zeta potential values are given in Fig3. The best possible condition of dispersion was identified at pH=9 and the silica IEP (IsoElectric Point) was determined at pH=2. Values situated on a zeta stable tray between pH=7 and pH=11, and makes the control of its state of dispersion easier. The dispersal of both sizes of silica was performed. The silica dispersions have been confirmed by ESEM micrographs. A technique of drop pulling on a glass support with an optical paper, according to a previous work in the laboratory [54], was used. Micrographs (Fig3) confirm and pH=3, silica particles showed an obvious tendency to form agglomerates. At pH=9, particles dispersion is clearly improved. Nevertheless, some agglomerates remain due to the Van Der Waals interactions between particles. It will be a challenge to

overcome these interactions and to find the best way during the process to improve dispersion of these agglomerates.

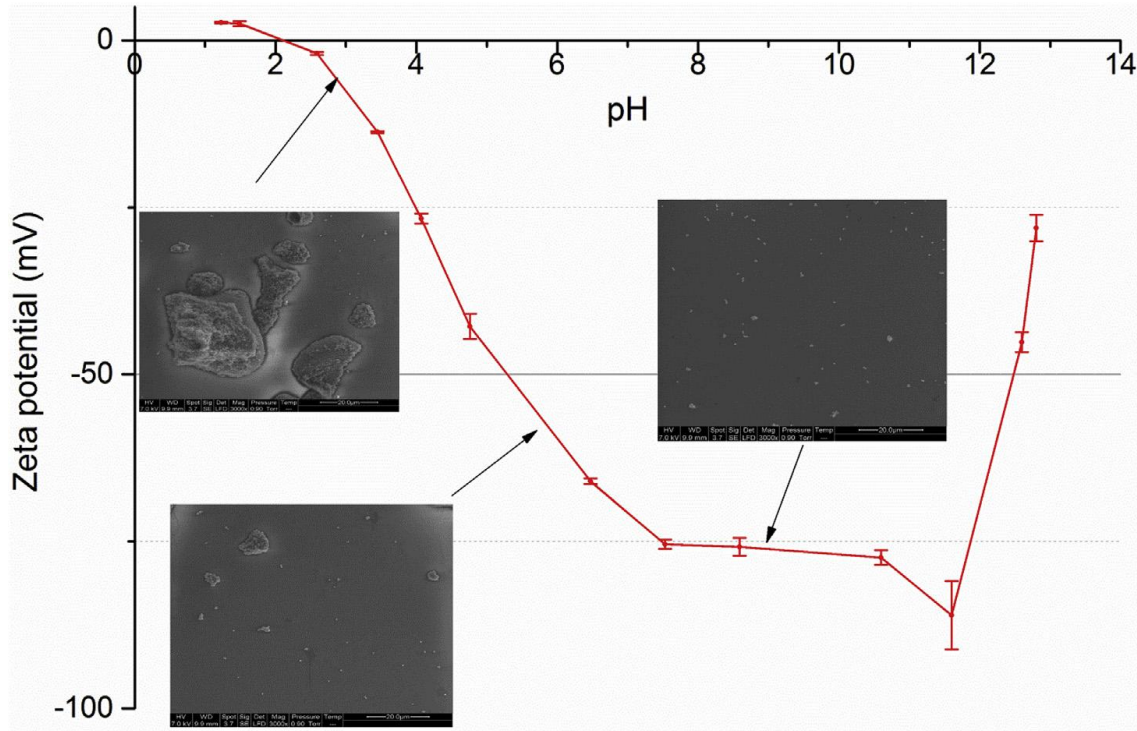


*Fig3. Zeta potential vs pH of synthesized silica.*

## 2. Elaboration process: influence on the dispersion

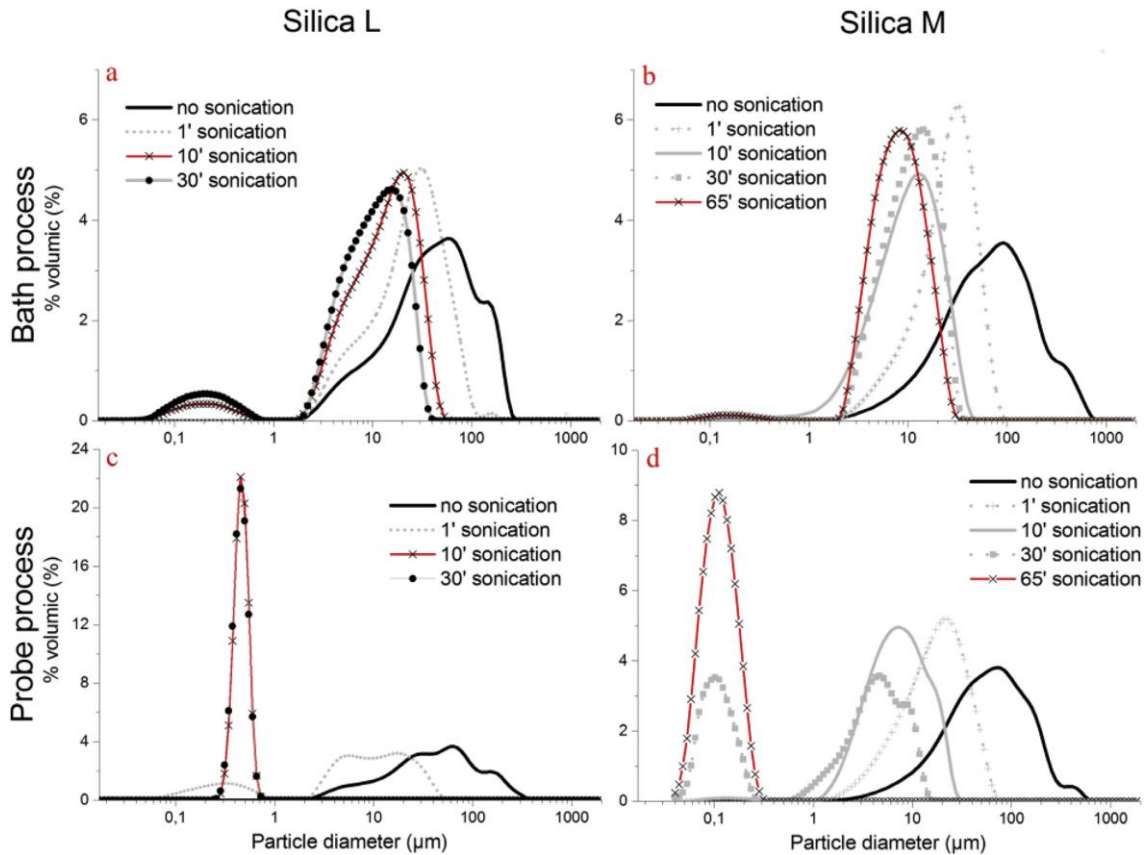
### 2.1 Suspension dispersion

A study on the sonication time required for the improvement of NPs dispersion in suspension was performed with laser granulometry and illustrated in Fig4. The statistical measure values are reported Table1.  $d_{max}$  is the biggest size in suspension and principal mode the most represented size in suspension. The two processes of dispersions (bath and probe process describe part I.4.1) have been investigated and compared. A monodisperse size distribution with the probe process after 10 and 65 minutes respectively for the silica L and silica M was observed. As expected, silica L needs less time of sonication to be dispersed. Indeed, the smaller the particle, the more difficult it is to disperse. With the bath process the same conditions have been applied but the monodisperse peak corresponding to an absence of agglomerates was not obtained. Agglomerates around 10-50  $\mu m$  were still present in the solution at the end of this sonication time.

According to the DLVO<sup>1</sup> theory [55], thermal agitation induces a stable state of the particles and cause the agglomeration of the system. For the same sonication time, probe process induces a better dispersion than bath process. It could be expected that probe process leads to a better dispersion into the composite in comparison with the bath process. With probe process the principal mode is shift towards the individual particle size without second mode. On the other hand, with bath process, the main mode always remains the same despite the appearance of a secondary mode representing approximately the size of a single particle.

Process		Principal mode ( $\mu\text{m}$ )	Second mode ( $\mu\text{m}$ )	$d_{\text{max}}$ ( $\mu\text{m}$ )
Bath	Silica L	20.70	0.25	63.41
	Silica M	8.15	0.148	36.24
Probe	Silica L	0.45	none	0.79
	Silica M	0.11	none	0.38

Table1. Laser granulometry: statistical measure values after sonication during 10 minutes for silica L and 65 minutes for silica M.



<sup>1</sup> Boris Derjaguin, Lev Landau, Evert Verwey and Theodoor Overbeek

*Fig4. Size distribution of NPs by laser granulometry in acetone of a) silica L/bath process b) silica M/bath process c) silica L/probe process and d) silica M/probe process.*

## **2.2 Master-batch dispersion**

In Fig5, the microstructures of master-batch PMMA/silica L (top) and PMMA/silica M (bottom) obtained with bath (left) and probe (right) processes with the require sonication time (determine previously, 10min for silica L and 65min for silica M) are illustrated. The fracture surface observation of the composite confirms the results obtained by laser granulometry. A real improvement of NPs distribution into the PMMA matrix can be observed in the case of probe process. It can be concluded that unlike the bath process, the probe process allows obtaining a homogenous composite. PMMA/silica obtained by bath process exhibits a large number of agglomerates between 10  $\mu\text{m}$  to 50  $\mu\text{m}$  diameter in the composite (approximately the same order size than agglomerates found Fig4). In this last case, it would be appropriate to consider that the composite produced is closer to a micro-structure than to a nano-structure. This kind of morphology should impact the mechanical testing results.

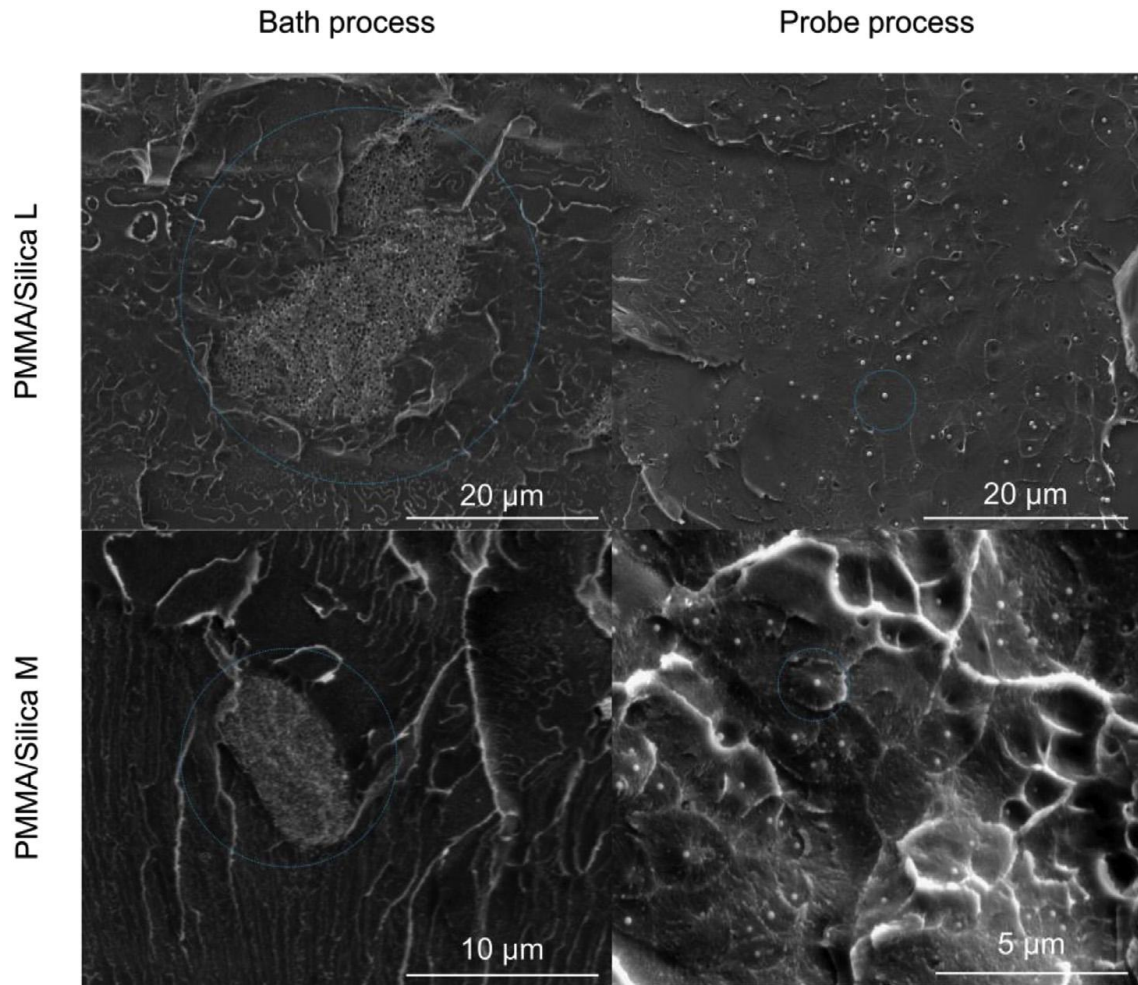


*Fig5.SEM topography micrographs: influence of the process on NPs distribution into the composite*

### 2.3 Strand dispersion

Aphelion™ 4.3.2 (ADCIS) software was used to quantify the observations performed on SEM micrographs obtained for the different PMMA/silica composites. The aim is to compare the influence of bath and probe processes on particles dispersion and to correlate size distribution obtained on the composite via images analysis and size distribution of the NPs in acetone. Results of this quantification analysis should indicate the possibility to obtain the silica NPs dispersion with the twin screw extrusion process. These results will also help to clarify importance of the preliminary dispersion process in suspension for the production of a well-dispersed composite.

SEM micrographs (Fig5) were binarized and NPs domains (around 1000 objects, to be statistically representative of the overall microstructure) were identified (red objects in Fig6), labeled and filtered by surface area value with respect to the scale of observation. The normalized volume frequency distribution is represented in Fig7 for both silica and



each preliminary process of dispersion, it is clear that independently of particles size, probe process leads to a better dispersion of fillers. This quantification confirms SEM observations.

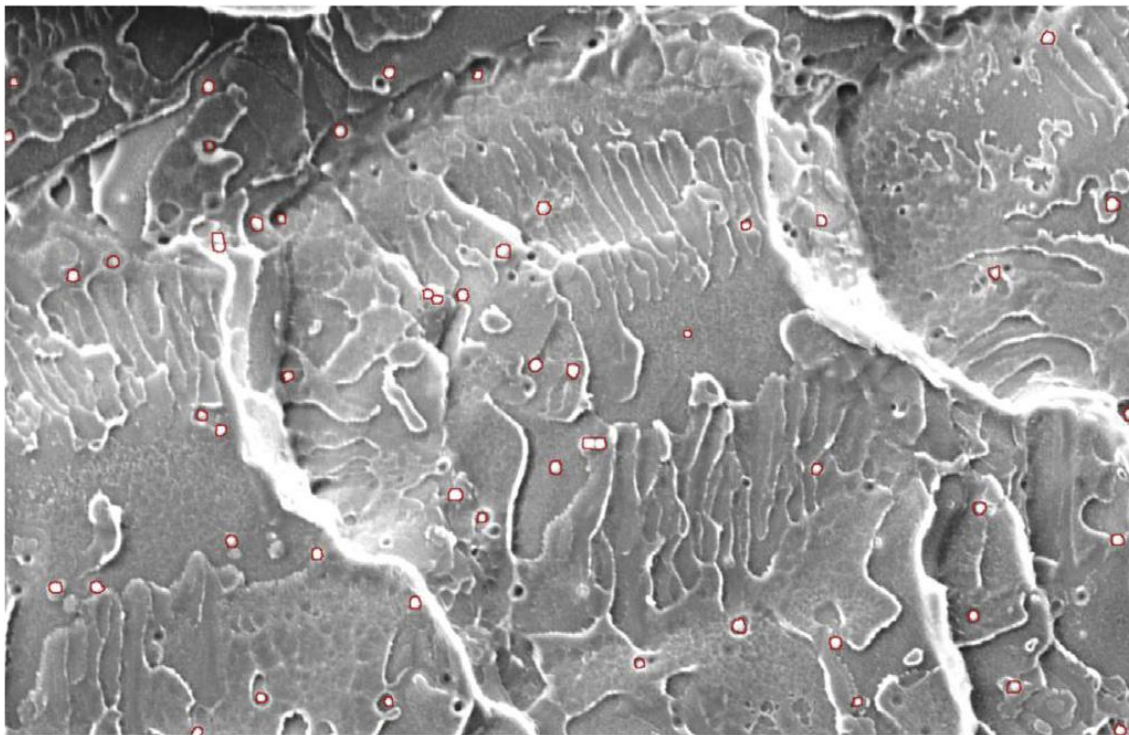


*Fig6.Object selection via Aphelion software*

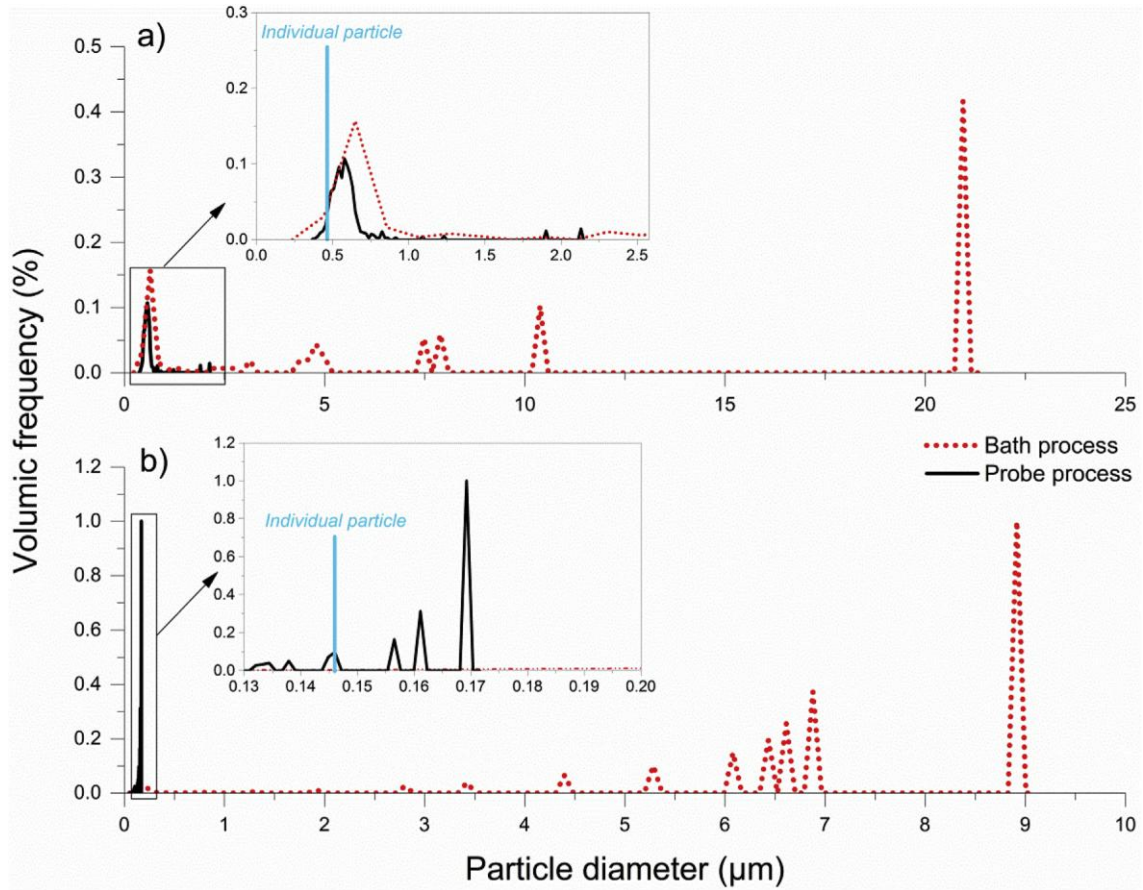


Fig7. Numerical granulometry via Aphelion software of composites a) PMMA/silica L with 10'' of sonication and b) PMMA/silica M with 65'' of sonication.

The granulometry deduced from SEM micrographs (Fig7), confirms the distribution measured by laser granulometry (Fig4) on the different suspensions (Table2). These results show that the second part of the process (concerning the dilution with twin-screw compounder) has little effect on the dispersion of the final composite. Indeed, the dilution step by twin-screw compounding had only an effect on the biggest agglomerates present into the master-batch. The distribution difference between laser granulometry in suspension and images treatment of composite is the shift of  $d_{max}$  with bath process. In fact, the applied energy during the compounding step is not sufficient to disperse the smallest agglomerates. These results demonstrated that pre-dispersion of NPs into the solvent process is the key for a good final dispersion of NPs into the system. It is important to note that silica has no tendency to re-agglomerate after the master-batch step.

Process		Principal mode ( $\mu\text{m}$ )	$d_{\text{max}}$ ( $\mu\text{m}$ )
Bath	Silica L	20.95	21.36
	Silica M	8.92	9.09
Probe	Silica L	0.58	2.13
	Silica M	0.161	0.17

Table2: quantitative granulometry by images treatment with Aphelion software

### 3. Mechanical properties

#### 3.1 Experiments

Uniaxial tensile tests were conducted to determine the mechanical properties (ultimate stress and Young's modulus) and to quantify the influence of the dispersion of NPs in the composites (Fig8).

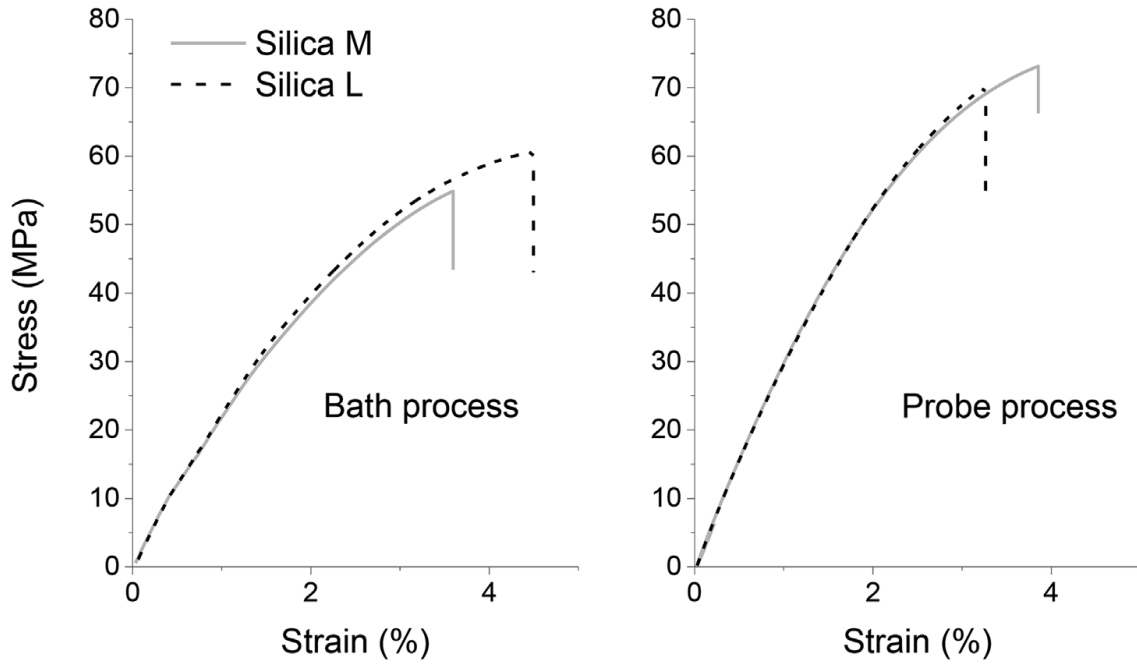
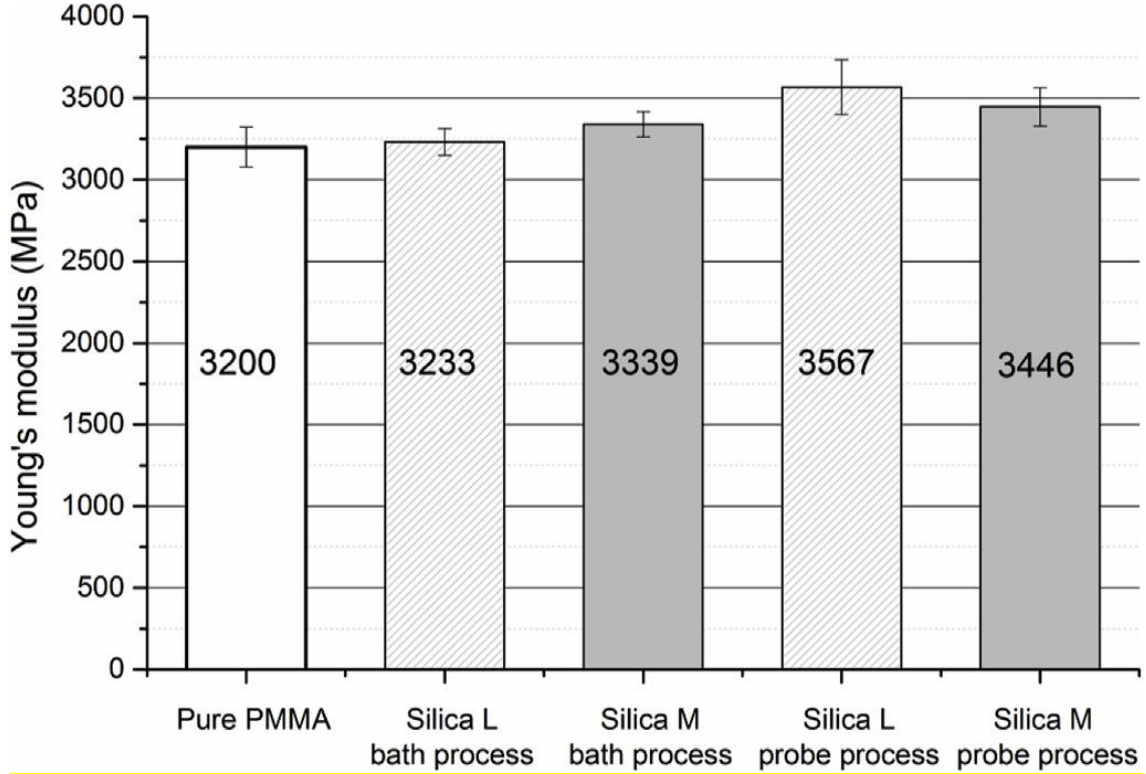


Fig8. Stress-strain curves of a) well-dispersed and b) poorly dispersed composites

As expected, the addition of well-dispersed particles in a PMMA matrix induces an increase in Young's modulus (Fig9) in comparison with the unfilled polymer. Fig9 shows that the composite obtained by probe process has higher mean Young's modulus, even though large scatter is observed for all the formulations. This improvement is probably due to the natural affinity between silica and PMMA. For bath process, silica L does not exhibit any reinforcing effect while PMMA with silica M particles has an



improvement of 4% in the Young's modulus. With probe process it was observed an improvement of 9% for both sizes. It is also interesting to note that, irrespective of the dispersion quality, the size effect on Young's modulus is negligible.



*Fig9. Process impact and size effect on Young's modulus*

This observation is not in contradiction with the well-known assumption that the smaller are the nanoparticles, the higher are the nanocomposites elastic properties. In the present study the particles are not really nanoparticles (their median diameter is larger than 100 nm) and their level of incorporation is much lower than traditional nanocomposites with low aspect ratio particles. A numerical study [56] confirms the absence of sensitivity of elastic parameters for spherical particles, incorporated at 1 vol%, with mean diameter value more than 10nm.

Concerning the ultimate properties, the associate standard deviation is lower for the probe process (Fig10), indicating that this process results in composites with less morphological defects. Indeed, in the bath process case, stresses have tendency to unchanged neat PMMA properties, for both particles sizes. In the contrary, ultimate stress has an increasing tendency for probe process case ( $\sim 21\%$  for silica L and  $\sim 26\%$  for silica M). These results confirm that a good dispersion leads to better mechanical properties.

A study on the relationship between dispersion metric and mechanical properties of PMMA/SWNT nanocomposites points out that the measured dispersion is crucial for reproducibility of mechanical properties [57].

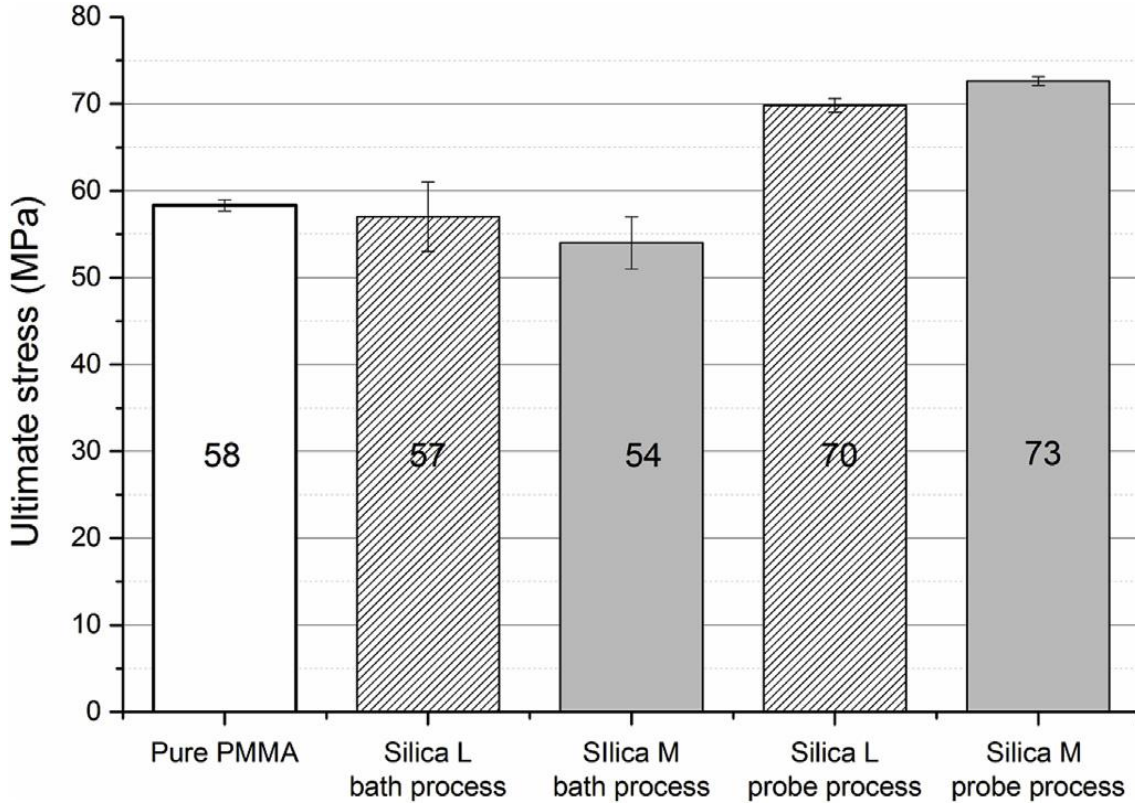


Fig10. Process impact and size effect on stress at break

### 3.2 Statistical analysis

A linear curve fit method was used to obtain the two Weibull parameters,  $\ln(-\ln((1 - P_r)))$  was plotted versus  $\ln \sigma_r$  and the best linear fit was computed (Fig.11). the  $R^2$  parameters (coefficients of determination) of neat PMMA and filled PMMA (M, L bath process and M, L probe process) are equal to 0.86, 0.90, 0.95, 0.77, 0.90 respectively. For the lastest composite (PMMA/ silica L well dispersed) the plot is non-linear which explains the low  $R^2$  coefficient (Fig.11). A bi-modal Weibull distribution could be more efficient in that case [58].

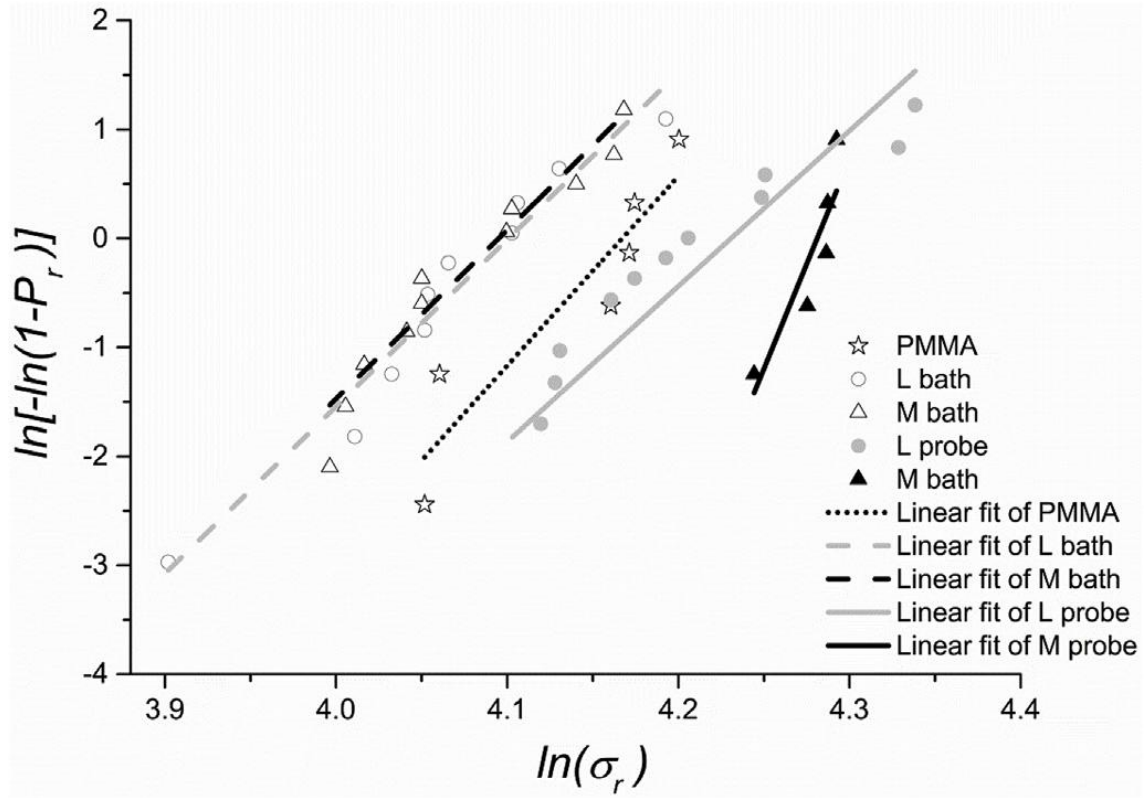


Fig.11. Accumulated Weibull probability plots for the failure stress, in MPa  
The Weibul parameters are given Table 3. These parameters are remarkably affected by the preparation process and composite microstructures.

	PMMA	L bath	M bath	L probe	M probe
m	17.4	15.3	17.6	14.5	24.7
$\sigma_0$ (MPa)	64.5	60.4	60.1	68.5	72.4

Table 3: Weibull parameters

In Table 3, it was observed that the Weibull parameter  $m$  increases with the probe process and only for the smallest particles. Higher value of this parameter indicates a more uniform strength distribution, as it is expected with an improvement of particle dispersion. This is consistent with the improvement of the average stresses at failure where the highest characteristic strength  $\sigma_0$  was obtained for the composite with the better particle dispersion. Besides, poor particle dispersion leads to the degradation of the characteristic strength in comparison with the native PMMA. This trend is clearly observed in Fig.11 with a cumulative probability density curve shifted towards right for probe process composites, and towards left for bath process composites. Besides, a size effect can be observed for well-dispersed silica composites where the predicted ultimate

stress for M probe process composites is higher than the stress for L probe process composites. This size effect does not exist for bath process composites.

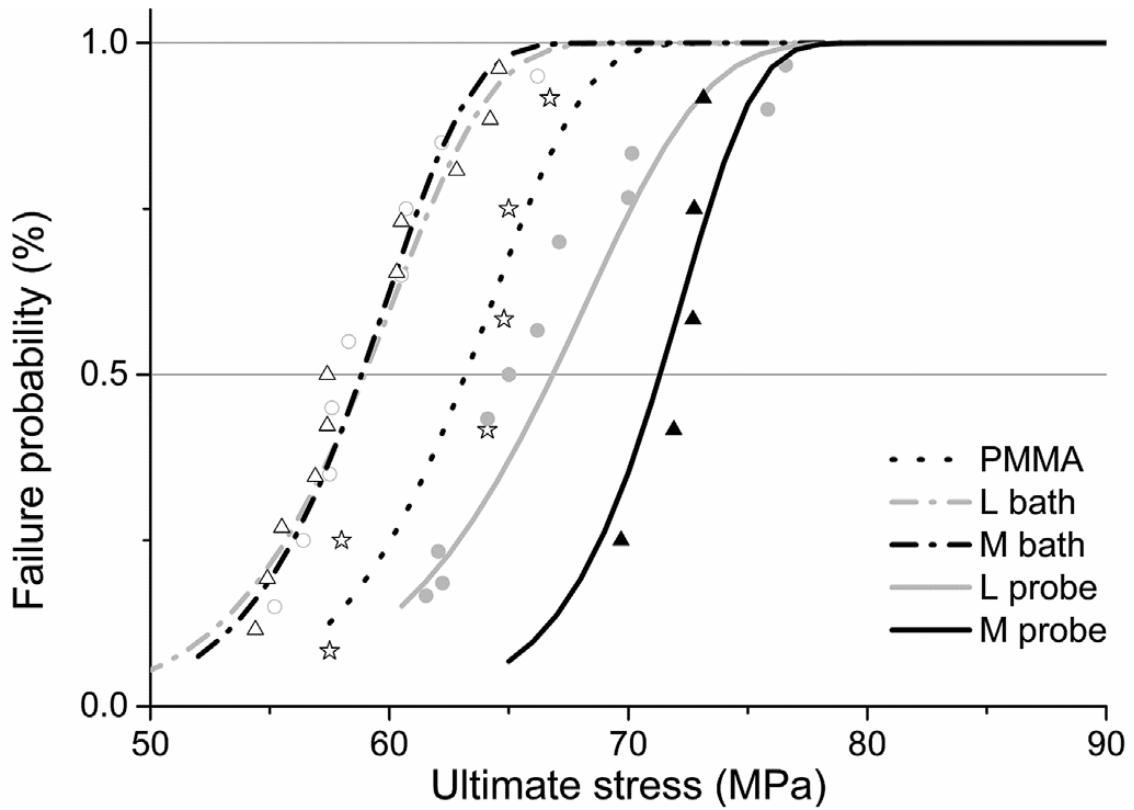


Fig.12. Weibull prediction

## Conclusion

This study allowed highlighting the importance to disperse particles before incorporation into the polymer matrix. It also highlights the link between particles size and difficulty to disperse. Finally, it shows that the phenomena of re-agglomeration are insignificant in our conditions of processing.

The second objective of this study was to bring out the influence of dispersion and size effect on the mechanical behavior of composites. Finally, a good dispersion of particles conduct to an improved Young's modulus and ultimate stress while a poor dispersion lead to an unmodified Young's modulus and a lower ultimate stress in comparison with native polymer matrix. Weibull analysis allowed to highlighting that a good dispersion shows a size effect contrary to poorly-dispersed composites.

The dispersion process developed for this study allowed obtaining the desired composites. However it was found thanks to the SEM micrographs that the interface between matrix and particles presented a lack of cohesion. It would be interesting to

work on a functionalization allowing the optimization of this interface between additive and matrix.

### **Acknowledgements**

This work was supported by the GDR Polynano and IMT mines Alès. The authors would like to thank Carine Joly Chivas, member of the GDR Polynano for the talks around the nanoparticles dispersion problematics.

Thanks are due to Jean-Claude Roux for the electronic microscopy.

### **References**

- [1] A. Dorigato, A. Pegoretti, Fracture behaviour of linear low density polyethylene-fumed silica nanocomposites, *Eng. Fract. Mech.* 79 (2012) 213–224.  
doi:10.1016/j.engfracmech.2011.10.014
- [2] R.M. Mutiso, K.I. Winey, Electrical Conductivity of Polymer Nanocomposites, *Polym Sci: A Compr Ref.* vol.7 (2012). doi:10.1016/B978-0-444-53349-4.00196-5
- [3] S.K. Kumar, R. Krishnamoorti, Nanocomposites: Structure, Phase Behavior, and Properties, *Annu. Rev. Chem. Biomol. Eng.* 1 (2010) 37–58. doi:10.1146/annurev-chembioeng-073009-100856
- [4] L. Nicolais, G. Carotenuto, Nanocomposites with tailored optical properties, *Multifunct. Polym. Compos.* 28 (2015) 842-857 doi:10.1016/B978-0-323-26434-1.00028-3
- [5] A. Dorigato, M. Sebastiani, A. Pegoretti, L. Fambri, Effect of Silica Nanoparticles on the Mechanical Performances of Poly(Lactic Acid), *J. Polym. Environ.* 20 (2012) 713–725. doi:10.1007/s10924-012-0425-6
- [6] Z. Fanglong, X. Qun, F. Qianqian, L. Rantong, L. Kejing, Influence of nano-silica on flame resistance behavior of intumescent flame retardant cellulosic textiles: Remarkable synergistic effect?, *Surf. Coatings Technol.* 294 (2016) 90–94.  
doi:10.1016/j.surfcoat.2016.03.059
- [7] A.A. Takashi Kashiwagi, Jeffrey W. Gilman, Kathryn M. Butler, Richard H. Harris, John R. Shields, Flame Retardant Mechanism of Silica Gel / Silica, *Fire Mater.* 24 (2000) 277–289. doi:2003612-172545
- [8] A.J. Crosby, J. Lee, Polymer Nanocomposites: The “Nano” Effect on Mechanical Properties, *Polym. Rev.* 47 (2007) 217–229.  
doi:10.1080/15583720701271278

- [9] L.Y. Matzui, L.L. Vovchenko, Y.S. Perets, O.A. Lazarenko, Electrical conductivity of epoxy resin filled with graphite nanoplatelets and boron nitride, *Materwiss. Werksttech.* 44 (2013) 254–258. doi:10.1002/mawe.201300117
- [10] Z. Tadmor, C.G. Gogos, *Principles of Polymer Processing*, 2nd ed., (2006) 322–408. ISBN: 978-0-471-38770-1
- [11] M. Barmouz, A. Araee, Effect of SiC Particles Dispersion on the Grain Size and Mechanical Properties of Cu/SiC Metal Matrix Nanocomposites Produced via MFSP, *J. Nano Res.* 26 (2013) 53–58. doi:10.4028/www.scientific.net/JNanoR.26.53
- [12] P. Chandran, T. Sirimuvva, N. Nayan, A.K. Shukla, S.V.S.N. Murty, S.L. Pramod, S.C. Sharma, S.R. Bakshi, Effect of carbon nanotube dispersion on mechanical properties of aluminum-silicon alloy matrix composites, *J. Mater. Eng. Perform.* 23 (2014) 1028–1037. doi:10.1007/s11665-013-0835-1
- [13] H. Fujiwara, S. Hamanaka, S. Kawamori, H. Miyamoto, Effect of Microstructure on the Mechanical Properties of Magnesium Composites Containing Dispersed Alumina Particles Prepared Using an MM / SPS Process, *Mat. Trans.* 55 (2014) 543–548. doi: 10.2320/matertrans.Y-M2013845
- [14] T. Ramanathan, S. Stankovich, D.A. Dikin, H. Liu, H. Shen, S.T. Nguyen, L.C. Brinson, Graphitic Nanofillers in PMMA Nanocomposites—An Investigation of Particle Size and Dispersion and Their Influence on Nanocomposite Properties, *J. Polym. Sci. Part B: Polym. Phys.* 45 (2007) 1390–1398. doi: 10.1002/polb.21187
- [15] Y. Zare, K.Y. Rhee, D. Hui, Influences of nanoparticles aggregation/agglomeration on the interfacial/interphase and tensile properties of nanocomposites, *Compos. Part B: Eng.* 122 (2017) 41–46. doi:10.1016/j.compositesb.2017.04.008
- [16] A. Dorigato, A. Pegoretti, L. Fambri, M. Slouf, J. Kolarik, Cycloolefin Copolymer/Fumed Silica Nanocomposites, *J. of Applied Polymer Sci.* 119 (2011) 3393–3402.
- [17] A. Golbang, M.H.N. Famili, M.M.M. Shirvan, A method for quantitative characterization of agglomeration degree in nanocomposites, *Compos. Sci. Technol.* 145 (2017) 181–186. doi:10.1016/j.compscitech.2017.04.013
- [18] A. Tessema, D. Zhao, J. Moll, S. Xu, R. Yang, C. Li, S.K. Kumar, A. Kidane, Effect of filler loading, geometry, dispersion and temperature on thermal conductivity of polymer nanocomposites, *Polym. Test.* 57 (2017) 101–106. doi:10.1016/j.polymertesting.2016.11.015

- [19] F. V. Ferreira, W. Francisco, B.R.C. Menezes, F.S. Brito, A.S. Coutinho, L.S. Cividanes, A.R. Coutinho, G.P. Thim, Correlation of surface treatment, dispersion and mechanical properties of HDPE/CNT nanocomposites, *Appl. Surf. Sci.* 389 (2016) 921–929. doi:10.1016/j.apsusc.2016.07.164
- [20] J.K. Ahmed, M.H. Al-maamori, H.M. Ali, Effect of nano silica on the mechanical properties of Styrene-butadiene rubber ( SBR ) composite, *Int. J. Mater. Sci. Appl.* 4 (2015) 15–20. doi:10.11648/j.ijmsa.s.2015040201.14
- [21] H. Shin, K. Baek, J.-G. Han, M. Cho, Homogenization analysis of polymeric nanocomposites containing nanoparticulate clusters, *Compos. Sci. Technol.* 138 (2017) 217–224. doi:10.1016/j.compscitech.2016.11.021
- [22] W.S. Junior, T. Emmeler, C. Abetz, U.A. Handge, J.F. dos Santos, S.T. Amancio-Filho, V. Abetz, Friction spot welding of PMMA with PMMA/silica and PMMA/silica-g-PMMA nanocomposites functionalized via ATRP, *Polymer* 55 (2014) 5146–5159. doi:10.1016/j.polymer.2014.08.022
- [23] J.L.H. Chau, C.C. Hsieh, Y.M. Lin, A.K. Li, Preparation of transparent silica-PMMA nanocomposite hard coatings, *Prog. Org. Coatings.* 62 (2008) 436–439. doi:10.1016/j.porgcoat.2008.02.005
- [24] V. Raji Vijay, A.M. Anitha, A.R. Ravindranatha Menon, Studies on blends of natural rubber and butadiene rubber containing silica-Organomodified kaolin hybrid filler systems, *Polymer* 89 (2016) 135–142. doi:10.1016/j.polymer.2016.02.037
- [25] M.R. Pourhossaini, M. Razzaghi-Kashani, Effect of silica particle size on chain dynamics and frictional properties of styrene butadiene rubber nano and micro composites, *Polymer* 55 (2014) 2279–2284. doi:10.1016/j.polymer.2014.03.026
- [26] H.S. Varol, M.A. Sánchez, H. Lu, J.E. Baio, C. Malm, N. Encinas, M.R.B. Mermet-Guyennet, N. Martzel, D. Bonn, M. Bonn, T. Weidner, E.H.G. Backus, S.H. Parekh, Multiscale effects of interfacial polymer confinement in silica nanocomposites, *Macromolecules.* 48 (2015) 7929–7937. doi:10.1021/acs.macromol.5b01111
- [27] T. Kang, J.H. Lee, S.-G. Oh, Dispersion of surface-modified silica nanoparticles in polyamide-imide (PAI) films for enhanced mechanical and thermal properties, *J. Ind. Eng. Chem.* 46 (2017) 289–297. doi:10.1016/j.jiec.2016.10.042
- [28] F. Wu, B. Zhang, W. Yang, Z. Liu, M. Yang, Inorganic silica functionalized with PLLA chains via grafting methods to enhance the melt strength of PLLA/silica nanocomposites, *Polymer* 55 (2014) 5760–5772. doi:10.1016/j.polymer.2014.08.070

- [29] Y. Feng, W. Zhang, G. Cui, J. Wu, W. Chen, Effects of the extrusion temperature on the microstructure and mechanical properties of TiBw/Ti6Al4V composites fabricated by pre-sintering and canned extrusion, *J. Alloys Compd.* 721 (2017) 383–391. doi:10.1016/j.jallcom.2017.05.309
- [30] Y. Cai, P. Hou, X. Cheng, P. Du, Z. Ye, The effects of nanoSiO<sub>2</sub> on the properties of fresh and hardened cement-based materials through its dispersion with silica fume, *Constr. Build. Mater.* 148 (2017) 770–780. doi:10.1016/j.conbuildmat.2017.05.091
- [31] S. Kawashima, J.-W.T. Seo, D. Corr, M.C. Hersam, S.P. Shah, Dispersion of CaCO<sub>3</sub> nanoparticles by sonication and surfactant treatment for application in fly ash–cement systems, *Mater. Struct.* 47 (2014) 1011–1023. doi:10.1617/s11527-013-0110-9
- [32] A. Hasani Baferani, A.A. Katbab, A.R. Ohadi, The role of sonication time upon acoustic wave absorption efficiency, microstructure, and viscoelastic behavior of flexible polyurethane/CNT nanocomposite foam, *Eur. Polym. J.* 90 (2017) 383–391. doi:10.1016/j.eurpolymj.2017.03.042
- [33] E. Manias, G. Polizo, H. Nakajima, M.J. Heidecker, *Fundamentals of Polymer Nanocomposite Technology, Flame Retardant Polymer Nanocomposites 1*, (2006) 31–66. doi:10.1002/9780470109038.ch2
- [34] L. Banks-Sills, D.G. Shiber, V. Fourman, R. Eliasi, A. Shlayer, Experimental determination of mechanical properties of PMMA reinforced with functionalized CNTs, *Compos. Part B: Eng.* 95 (2016) 335–345. doi:10.1016/j.compositesb.2016.04.015
- [35] P. Jindal, M. Sain, N. Kumar, Mechanical Characterization of PMMA/MWCNT Composites Under Static and Dynamic Loading Conditions, *Mater. Today Proc.* 2 (2015) 1364–1372. doi:10.1016/j.matpr.2015.07.055
- [36] F.A. Alzarrug, M.M. Dimitrijević, R.M. Jančić Heinemann, V. Radojević, D.B. Stojanović, P.S. Uskoković, R. Aleksić, The use of different alumina fillers for improvement of the mechanical properties of hybrid PMMA composites, *Mater. Des.* 86 (2015) 575–581. doi:10.1016/j.matdes.2015.07.069
- [37] F. Fallah, M. Khorasani, M. Ebrahimi, Improving the mechanical properties of waterborne nitrocellulose coating using nano-silica particles, *Prog. Org. Coatings.* 109 (2017) 110–116. doi:10.1016/j.porgcoat.2017.04.016
- [38] D.W. McCarthy, J.E. Mark, D.W. Schaefer, Synthesis, structure, and properties of hybrid organic-inorganic composites based on polysiloxanes. I. Poly(dimethylsiloxane) elastomers containing silica, *J. Polym. Sci. Part B: Polymer*



Phys. 36 (1998) 1167–1189. doi:10.1002/(sici)1099-0488(199805)36:7<1167::aid-polb7>3.0.co;2-r

[39] D.N. Bikiaris, G.Z. Papageorgiou, E. Pavlidou, N. Vouroutzis, P. Palatzoglou, G.P. Karayannidis, Preparation by melt mixing and characterization of isotactic polypropylene/SiO<sub>2</sub> nanocomposites containing untreated and surface-treated nanoparticles, *J. Appl. Polym. Sci.* 100 (2006) 2684–2696. doi:10.1002/app.22849

[40] H. Zou, S. Wu, J. Shen, Polymer / Silica Nanocomposites : Preparation , Characterization , Properties , and, *Chem. Rev.* 108 (2008) 3893–3957. doi:10.1021/cr068035q

[41] J. Yuan, S. Zhou, G. Gu, L. Wu, Effect of the particle size of nanosilica on the performance of epoxy/silica composite coatings, *J. Mater. Sci.* 40 (2005) 3927–3932. doi:10.1007/s10853-005-0714-8

[42] A.S. Blivi, F. Benhui, J. Bai, D. Kondo, F. B?doui, Experimental evidence of size effect in nano-reinforced polymers: Case of silica reinforced PMMA, *Polym. Test.* 56 (2016) 337–343. doi:10.1016/j.polymertesting.2016.10.025

[43] T. Adachi, W. Araki, M. Higuchi, Mixture law including particle-size effect on fracture toughness of nano- and micro-spherical particle-filled composites, *Acta Mech.* 214 (2010) 61–69. doi:10.1007/s00707-010-0314-9

[44] J. Cho, M.S. Joshi, C.T. Sun, Effect of inclusion size on mechanical properties of polymeric composites with micro and nano particles, *Compos. Sci. Technol.* 66 (2006) 1941–1952. doi:10.1016/j.compscitech.2005.12.028

[45] T. Parpaite, B. Otazaghine, A. Taguet, R. Sonnier, A.S. Caro, J.M. Lopez-Cuesta, Incorporation of modified Stöber silica nanoparticles in polystyrene/polyamide-6 blends: Coalescence inhibition and modification of the thermal degradation via controlled dispersion at the interface, *Polymer* 55 (2014) 2704–2715. doi:10.1016/j.polymer.2014.04.016

[46] T. Parpaite, B. Otazaghine, A.S. Caro, A. Taguet, R. Sonnier, J.M. Lopez-Cuesta, Janus hybrid silica/polymer nanoparticles as effective compatibilizing agents for polystyrene/polyamide-6 melted blends, *Polymer* 90 (2016) 34–44. doi:10.1016/j.polymer.2016.02.044

[47] K.S. Rao, K. El-Hami, T. Kodaki, K. Matsushige, K. Makino, A novel method for synthesis of silica nanoparticles, *J. Colloid Interface Sci.* 289 (2005) 125–131. doi:10.1016/j.jcis.2005.02.019

- [48] L. Chen, Z. Xu, H. Dai, S. Zhang, Facile synthesis and magnetic properties of monodisperse Fe<sub>3</sub>O<sub>4</sub>/silica nanocomposite microspheres with embedded structures via a direct solution-based route, *J. Alloys Compd.* 497 (2010) 221–227.  
doi:10.1016/j.jallcom.2010.03.016
- [49] A. K. Nozawa, H. Gailhanou, L. Raison, P. Panizza, H. Ushiki, E. Sellier, J. P. Delville, M.H. Delville, Smart Control of Monodisperse Stöber Silica Particles: Effect of Reactant Addition Rate on Growth Process, *Langmuir*. 21 (2005) 1516–1523.  
doi:10.1021/LA048569R
- [50] Weibull W. A Statistical Distribution Function of Wide Applicability. *J Appl Mech* 1951:293–7.
- [51] C.O. Metin, L.W. Lake, C.R. Miranda, Q.P. Nguyen, Stability of aqueous silica nanoparticle dispersions, *J. Nanoparticle Res.* 13 (2011) 839–850. doi:10.1007/s11051-010-0085-1
- [52] M.K. Poddar, S. Sharma, V.S. Moholkar, Investigations in two-step ultrasonic synthesis of PMMA/ZnO nanocomposites by in-situ emulsion polymerization, *Polymer* 99 (2016) 453–469. doi:10.1016/j.polymer.2016.07.052
- [53] and W.T. Rahul P. Bagwe, Lisa R. Hilliard, Surface Modification of Silica Nanoparticles to Reduce Aggregation and Nonspecific Binding, *Langmuir*. 22 (2006) 4357–4362. doi:10.1021/la052797j
- [54] C. Autier, N. Azema, J.-M. Taulemesse, L. Clerc, Mesostructure evolution of cement pastes with addition of superplasticizers highlighted by dispersion indices, *Powder Technol.* 249 (2013) 282–289. doi:10.1016/j.powtec.2013.08.036
- [55] M. Elimelech, J. Gregory, X. Jia et al. *Particle Deposition and Aggregation: Measurement, Modeling, and Simulation* (1995). ISBN: 978-0-7506-7024-1
- [56] R. D. Peng, H. W. Zhou, H. W. Wang, and L. Mishnaevsky. Modeling of nano-reinforced polymer composites: Microstructure effect on Young's modulus, *Comput. Mater. Sci.*, 60 (2012) 19–31. doi:10.1016/j.commatsci.2012.03.010
- [57] T. Kashiwagi, J. Fagan, J.F. Douglas, K. Yamamoto, A.N. Heckert, S.D. Leigh, J. Obrzut, F. Du, S. Lin-Gibson, M. Mu, K.I. Winey, R. Haggemueller, Relationship between dispersion metric and properties of PMMA/SWNT nanocomposites, *Polymer* 48 (2007) 4855–4866. doi:10.1016/j.polymer.2007.06.015
- [58] Y. Zhou, F. Pervin, V.K. Rangari, S. Jeelani, Fabrication and evaluation of carbon nano fiber filled carbon/epoxy composite, *Mater. Sci. Eng. A.* 426 (2006) 221–228. doi:10.1016/j.msea.2006.04.031